Magnetically Driven Growth of Anthracene Thin Films by Organic Molecular Beam Deposition

A. Sassella,* I. Baldi, A. Borghesi, M. Campione, L. Miozzo, M. Moret, A. Papagni, A. Salerno, S. Tavazzi, and S. Trabattoni

INFM and Department of Materials Science, Università di Milano-Bicocca, Via R. Cozzi 53, I-20125 Milano, Italy

Received: September 29, 2004; In Final Form: December 15, 2004

The possible use of a static magnetic field during organic molecular beam deposition of thin molecular films for inducing some preferential growth is discussed and the magnetic properties of diamagnetic molecules and molecular crystals are recalled. Considering prototypical materials, namely anthracene molecules and potassium phthalate substrates, which interact and may give rise to polycrystalline films with specific orientations, we show that in the presence of a magnetic field the films display a macroscopic preferential orientation as a result of minimization of the magnetic energy contribution. A very good agreement between the results of optical spectroscopy, atomic force microscopy, and predictions made on the basis of the anisotropic magnetic susceptibility of anthracene is found.

Introduction

The growth of thin films of organic molecular materials by organic molecular beam deposition (OMBD[1]) is having a great expansion because it permits, with respect to other techniques, a higher control of the sample quality in terms of composition uniformity, morphology, structure, and, therefore, optical and transport properties. Among the growth parameters useful for such a control and tuning of the properties, the type and temperature of the substrate are of fundamental importance, together with the pressure in the growing chamber and the source temperature. Also external electric or magnetic fields can be useful, which can rather easily be applied during OMBD, adding some contribution in driving the nucleation and growth of the films. This is particularly important for physisorbed materials, such as molecular materials, or when inert substrates are employed, because the weak interactions between the deposited molecules and the substrate surface are not always sufficient to obtain a film with a high degree of order. Several studies have been carried out on the growth of molecular single crystals under magnetic field, where the balance between magnetic and gravitational energy contributions to the growing crystals is discussed and some results on field-induced orientation and morphology of the crystals presented.[2−6] Recently, a magnetic field has been also used to drive the vacuum growth of molecular conjugated thin films,[7,8] even if its effect on the film structure and morphology has not been discussed in details. In fact, morphology is likely to be the most sensitive parameter, because the strong anisotropy of the magnetic susceptibility of most conjugated molecules may lead to an orienting effect of the magnetic field, which in turn may directly influence the shape, size, and orientation of the crystallites usually constituting the thin films.

In general, when subjected to a magnetic field, a molecule varies its energy by $E_B = -\mathbf{m}\cdot\mathbf{B}$, where **B** is the magnetic induction field and **m** is the total molecular magnetic moment; for a diamagnetic molecule, **m** reduces to the induced moment (Larmor contribution), opposite to the field, so that $E_B = mB$ is always a destabilizing positive contribution.[9] When the magnetic response is anisotropic, i.e., the magnetic moment varies with the orientation of the external field with respect to the molecule, and the molecule is free to move, it tends to orient itself in the field to minimize E_B. Usually the magnetic properties of crystals are expressed in terms of the dimensionless volume susceptibility $\chi = \mathbf{M}/\mathbf{H}$, with **H** the magnetic field and **M** the macroscopic magnetization; χ accounts for the magnetic response of the crystal, being negative for diamagnetic compounds. When anisotropic crystals are considered, the susceptibility is a diagonal tensor, so that three susceptibility values fully describe their magnetic behavior, namely χ_x, χ_y, and χ_z, for magnetic field aligned with the *x*, *y*, and *z* principal axes, respectively, of the tensor. For a molecule, an analogous definition of the molecular susceptibility *K* holds, being K_x, K_y, and K_z the values describing the response when the field is aligned with the principal inertia axes of the molecule *x*, *y*, and *z*. Given the crystal structure, the molecular direction cosines link the *K* and χ values, so that the magnetic response can be described using either the former or the latter ones. The magnetic energy contribution E_B can easily be rewritten using the diamagnetic susceptibility; in addition, because χ varies for different orientations of the field, also E_B varies:[9]

$$E_{Bj} = -\frac{\chi_j}{2\mu_0} V B_j^2 \qquad j = x, y, z \tag{1}$$

where μ_0 is the vacuum magnetic permeability, *V* is the volume of the crystal, and B_j is the field component along the *j* direction.

When the film deposition process is considered, the formation of the first crystal nuclei on the substrate is the result of a balance between several energy contributions. The free energy change ΔG for an aggregate undergoing a phase transition during heterogeneous nucleation can be written in the following form:[10]

$$\Delta G = -n_c \Delta\mu + \sum_j \gamma_j S_j + (\gamma_i - \beta) S_i \tag{2}$$

* Corresponding author. E-mail: adele.sassella@mater.unimib.it.

10.1021/jp045581j CCC: $30.25 © 2005 American Chemical Society
Published on Web 02/19/2005

The first term in eq 2 is the volume free energy term associated with the phase transition, because $\Delta\mu$ is the energy associated with the transfer of a molecule from the vapor to the infinite crystal (supersaturation), and n_c is the total number of molecules in the crystal nucleus. The sum of the second and last terms represents the surface free energy of the aggregate. When heterogeneous nucleation is considered, the interfaces present during nucleation are (a) the vapor/crystal interfaces, (b) the vapor/substrate interfaces, and (c) the substrate/crystal interfaces. The energy of the vapor/crystal interfaces is given by summing over all the interfaces j the products of the vapor/crystal interface energy of the j-th interface γ_j with its surface area S_j (second term in eq 2). The energy balance accounting for the formation of the substrate/crystal interface at the expense of the vapor/substrate interface is expressed by the last term of eq 2, where γ_i and S_i are the energy and surface area of the specific crystal face in contact with the substrate, respectively, and β is the specific surface energy of adhesion. The competition between negative volume terms and positive surface terms gives rise to a maximum of the free energy for some critical crystal nucleus size. Hence, except when the surface energy β exceeds the surface energy of the contact plane γ_i (which is strongly unlikely for weakly interacting molecules and substrates), nucleation is referred to as an activated process. The energy barrier for nucleation is lowered by a high supersaturation and a favorable interaction between the film nuclei and the substrate, expressed quantitatively by the parameter β. This can be achieved by selecting the contact plane of the crystalline aggregates which guarantees the highest adhesion, possibly by epitaxial matching along particular crystallographic directions.

When deposition is carried out in the presence of a static magnetic induction field B in the proximity of the substrate, an additional volume term, namely that of eq 1, must be considered in eq 2. Whatever the orientation of the crystalline aggregates, this term is positive for diamagnetic materials and then increases the energy for nucleation. Because the nucleation rate depends exponentially[10] on the energy barrier for nucleation (ΔG^*), as a first consequence, under the same deposition conditions but in the presence of a magnetic field, a diamagnetic compound should display a lower number of bigger nuclei. Furthermore, the presence of a magnetic field gradient above the substrate gives rise to a repulsive force acting on the impinging diamagnetic molecules, namely $F_B = m\nabla B$. This force is expected to reduce the deposition rate of molecules at the substrate level and then to contribute, together with the increment of the energy barrier for nucleation, to a lowering of the total amount of material deposited on the substrate. Another effect of the magnetic field can be a peculiar orientation of the film nuclei on the substrate resulting from their tendency to orient following the minimum of the magnetic energy. Even in the case when the film/substrate contact plane is unchanged, the magnetic energy may be sufficient to drive the film azimuthal orientation or to make the film "choose" one of equivalent (in the absence of the magnetic field) preferential orientations.

Within this frame, we grew by OMBD thin films of anthracene (AN), a well-known compound fully characterized in terms of magnetic anisotropy. The growth is performed in the absence of magnetic field and under a static magnetic field in different configurations, while the other parameters were kept constant (substrate and source temperatures, vacuum level, substrate, and deposition time), to check the field effects. (010)-oriented potassium acid phthalate (KAP) was chosen as substrate for its affinity with the conjugated molecules, being an organic single crystal with aromatic rings, therefore inducing some preferential film orientations. The influence of the magnetic field on the surface morphology and on the structure of the films is investigated by atomic force microscopy (AFM) and polarized optical transmission spectroscopy and discussed.

Materials and Methods

Thin films of commercial anthracene[11] were deposited by OMBD[1,12] under a pressure below 10^{-7} Torr, after purification of the starting material by sublimation. Slabs of freshly cleaved (010)-oriented KAP[13] were used as substrates. Film growth was carried out at 70 °C source temperature using a Knudsen effusion cell and mounting the substrates on the coldfinger of a liquid N_2 cryostat to minimize desorption during film growth; the estimated substrate temperature during OMBD is about 80 K. Several samples were grown under exactly the same conditions, but without any magnetic field or with a static magnetic field of 0.2 T intensity applied along different crystal directions of the substrate surface, or perpendicular to it, by mounting the substrate close to a disk magnet 1 cm in diameter properly oriented on the sample holder. The amount of material deposited (or film nominal thickness) is usually monitored in-situ by a quartz microbalance close to the substrate;[14] here, anthracene being highly volatile and therefore the microbalance reliability being limited, all the samples were prepared by maintaining the same deposition time. Normal incidence optical transmission measurements were carried out in the spectral range from 2 to 4.2 eV with linearly polarized light using a spectrometer Perkin-Elmer Lambda 900 equipped with a depolarizer and Glann Taylor calcite polarizers. AFM measurements were carried out using a Digital instrument Nanoscope IIIa on all the samples at both low and high (molecular) resolution to study their surface morphology and structure as a function of the different growth conditions. The number of islands per unit surface (island density number) was evaluated counting directly in the images the number of separated nuclei for the thinnest samples or individuating the number of units in clustered nuclei for the thickest ones. A fast Fourier analysis of the contrast of high-resolution images was used to get rid of the noise artifacts, then identifying the unit cell parameters of the surface lattice.

Results

In Figure 1 the AN molecular structure and crystal unit cell are illustrated, the directions corresponding to the principal susceptibility values indicated and both the K and χ literature values reported.[15] In addition, in Figure 1c a sketch of the geometry to be considered for evaluating the effective susceptibility for different orientations of AN crystallites on KAP in the presence of the magnetic field is reported.

The AN thin films grown on KAP(010) under different magnetic field configurations were studied by optical absorption and AFM. Figure 2 shows the absorbance spectra collected with polarized light on three samples grown under the same conditions and with the same deposition time without any magnetic field (a), with a magnetic field $B = 0.2$ T along the [100] or a_{KAP} direction of the KAP substrate (b), and with a magnetic field $B = 0.2$ T along the [001] or c_{KAP} direction of the substrate (c). The spectra of the samples grown under a magnetic field perpendicular to the substrate are not reported, being completely equivalent to those in Figure 2b, except for a nearly double intensity.

Figure 3 reports AFM images of three films of AN deposited by OMBD under the same conditions: no field [(a) and (b)],

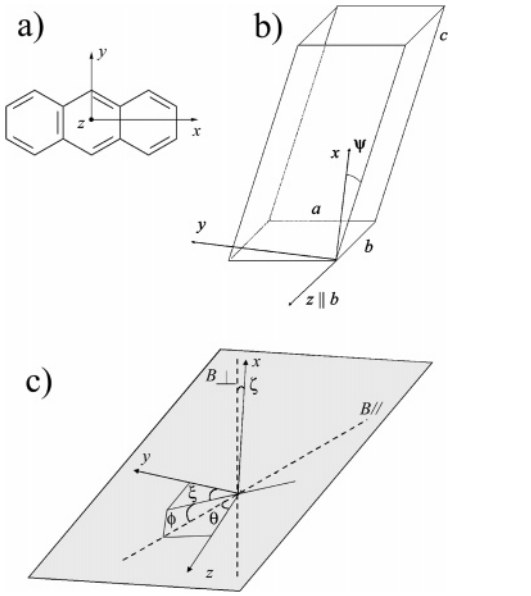

Figure 1. (a) Molecular structure of AN (H atoms are omitted). (b) Monoclinic unit cell of the AN single crystal,[16] with $a = 8.553$ Å, $b = 6.016$ Å, $c = 11.172$ Å, and $\beta = 124.60°$. For the molecule, the directions *x*, *y*, and *z* correspond to the molecular susceptibility values[15] $K_x = -9.66 \times 10^{-4}$ cm^3 mol^{-1}, $K_y = -9.64 \times 10^{-4}$ cm^3 mol^{-1}, and $K_z = -31.3 \times 10^{-4}$ cm^3 mol^{-1}. For the crystal, *x*, *y*, and *z* are the principal axes of the susceptibility tensor, where *x* and *y* lie in the *ac* plane of the crystal ($\psi = 8°$ for AN) and *z* is parallel to the monoclinic axis *b*; the χ values are[15] $\chi_x = -6.59 \times 10^{-6}$, $\chi_y = -18.6 \times 10^{-6}$, and $\chi_z = -9.05 \times 10^{-6}$. (c) Sketch of the method for evaluating the effective susceptibility for magnetic field directions parallel or perpendicular to the *ab* plane of AN; the gray plane contains both the B || field direction and the *z* axis and is drawn as a guide for the eye. $\zeta = 26.6°$ for any direction of B ||; in addition, $\xi = 90°$ $\phi = 0°$ when B || is along the b_{AN} direction, and $\xi = 0°$ $\phi = 26.6°$ when B || is along the a_{AN} direction (ϕ varies from 0° to 26.6° for directions of B || intermediate between b_{AN} and a_{AN}).

field parallel to a_{KAP} and c_{KAP} [(d) and (e), (g) and (h), respectively]. To obtain a film with $B = 0$ with well separated islands, a deposition with half the deposition time was also carried out. Figure 3b reports an AFM image of this film. The AFM analysis of the surface for films deposited under a magnetic field perpendicular to the substrate does not reveal any difference with respect to Figure 3a,b, therefore no images are reported here. Parts c, f, and i of Figure 3 report the orientations of the crystallites for films deposited with $B = 0$, B || a_{KAP}, and B || c_{KAP}, respectively. Finally, Figure 4 reports a 5×5 μm^2 AFM image of an AN film grown on KAP(010) with the magnetic field parallel to the c_{KAP} (a), the crystal morphology of AN drawn from the lattice parameters and considering the typical shape of bulk AN crystals[17] (b), and a 5×5 nm^2 filtered high-resolution AFM image showing the molecular arrangement at the surface of an AN crystallite (c).

From the AFM analysis a quantitative study of the island density number for the different samples (n_0 and n for $B = 0$ and $B \neq 0$, respectively) is carried out and the results are reported in Table 1, together with the values of the increment in the energy barrier for nucleation in the presence of magnetic field $\Delta(\Delta G^*)$, estimated from the n data (see the Discussion).

Discussion

The first characteristics of the optical spectra in Figure 2 is their close correspondence to the spectra of AN single crystals collected with light impinging on the (001) or on the $(20\bar{1})$ crystal faces,[18] whereas the response for light impinging on other

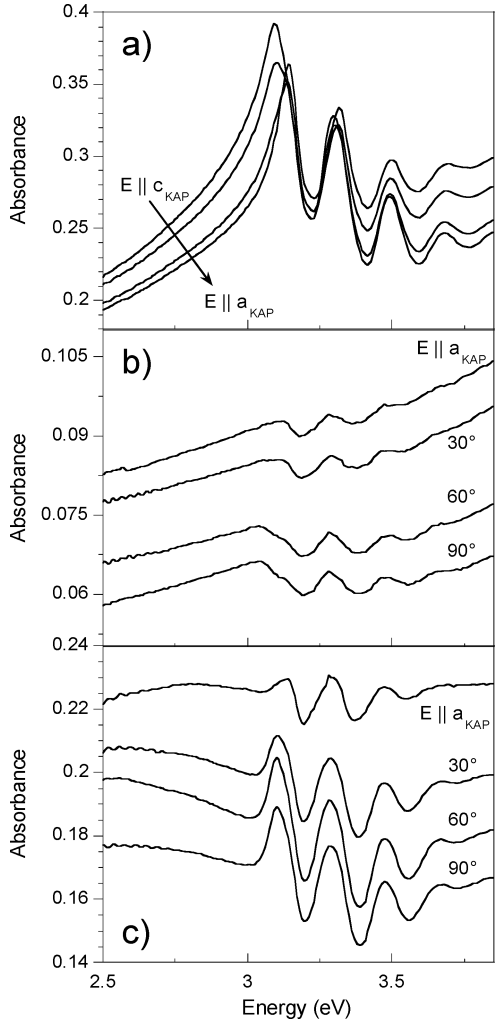

Figure 2. Absorbance spectra collected at normal incidence with electric field of the light linearly polarized along four different directions, in 30° steps from parallel to the *a* axis of KAP to parallel to the *c* axis of KAP, on three samples grown by OMBD under the same conditions and with the same deposition time; samples with the different magnetic field configurations during growth were analyzed: (a) no magnetic field, (b) magnetic field along the *a* direction of the KAP substrate, and (c) magnetic field along the *c* direction of the KAP substrate.

crystal planes is different. In particular, analyzing Figure 2a, where the peaks are more intense, the match of the spectral position and line shape indicates that the film is crystalline, with either the $(001)_{AN}$ or the $(20\bar{1})_{AN}$ as contact plane with $(010)_{KAP}$. Although they give a very similar optical response in this spectral range, we should note here that the lower symmetry of the $(20\bar{1})_{AN}$ plane with respect to the $(001)_{AN}$ makes the growth of the former less favored. The same spectrum, with a lower intensity, is clearly detected also in Figure 2 b) and c), indicating that the presence of the magnetic field during film growth does not change the KAP/AN contact plane.

The strong intensity difference observed in Figure 2 for the different samples, all with the same deposition time, confirms one of the effects of the magnetic field, which limits the quantity of deposited material through the repulsive force F_B and the increment of the energy barrier for nucleation. In particular, when B is parallel to the KAP surface (in particular the condition B || a_{KAP} is considered here, because when B || c_{KAP} the optical anisotropy also affects the peak intensity, therefore preventing a fully reliable comparison with the peak intensity in spectra collected on the other samples) the lowest intensity is detected

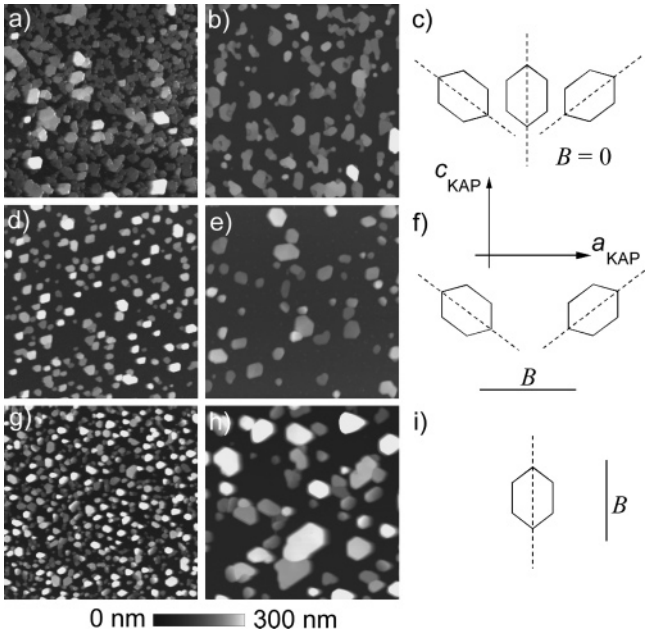

Figure 3. $30 \times 30\ \mu m^2$ (a, d, and g) and $10 \times 10\ \mu m^2$ (b, e, and h) AFM images of AN films grown on KAP(010) without any magnetic field (a and b), with an applied magnetic field parallel to the substrate either along the *a* axis of KAP (d and e), and parallel to the substrate and along the *c* axis of KAP (g and h). All samples were grown in the same conditions except the sample in (b) which was grown with half the deposition time. The orientation of crystallites is better visualized in (c), (f), and (i) where a schematic projection of their ab_{AN} plane on the substrate surface is reported for $B = 0$, $B \parallel a_{KAP}$, and $B \parallel c_{KAP}$, respectively. The dotted lines represent the b_{AN} axis.

and the amount of AN present on the substrate is therefore the lowest, being nearly half of that observed in the samples deposited under a magnetic field perpendicular to the substrate. This suggests that in the latter condition the AN molecules in the beam are subjected to a less intense magnetic force F_B, probably due to a weaker magnetic field gradient acting on the molecules under this configuration; indeed, the field intensity distribution around the magnet is broader along one direction and sharper perpendicularly.

A very important characteristics of the optical spectra is their dependence on light polarization, which demonstrates the anisotropy of the crystalline AN films. In turn, this depends on the magnetic properties of AN molecules and crystalline nuclei. Indeed, in the absence of magnetic field during deposition (see Figure 2a a very slight anisotropy is observed only on the peak at about 3.1 eV, with a ratio of about 1.1 between the maxima in the spectra collected with light polarized along a_{KAP} and c_{KAP}; this behavior matches with that of the single crystal,[18] where, however, the same ratio reaches the much higher value of 3.9, so that the orientation of the crystalline islands in this film can be considered nearly random. Some spectral shift of the same peak is also detected, which again recalls the single-crystal behavior, where a shift occurs with light polarization for the peaks in the spectra obtained on the $(001)_{AN}$ or the $(20\bar{1})_{AN}$ planes. Looking at Figure 2b, optical anisotropy is absent for the sample grown under a magnetic field parallel to a_{KAP}; similar conclusions hold for the spectra of the sample grown under a perpendicular magnetic field (not shown). On the contrary, a much different behavior is found in Figure 2c, where the magnetic field during OMBD was parallel to c_{KAP}: indeed, here all the peaks show a strong anisotropy, up to 3.6 for the peak at about 3.1 eV, and of about 2 for the other peaks at 3.3, 3.5, and 3.7 eV. The comparison with the single crystal spectra

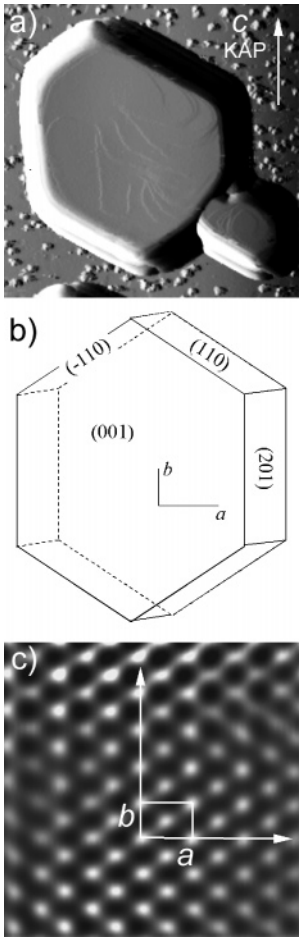

Figure 4. (a) $5 \times 5\ \mu m^2$ AFM image of an AN film grown on KAP(010) with the applied magnetic field parallel to the *c* axis of the KAP substrate. (b) Crystal morphology of AN drawn from the lattice parameters. (c) $5 \times 5\ nm^2$ filtered AFM image showing at molecular resolution the surface structure of the AN crystallite in (a).

TABLE 1: Influence of the Magnetic Field on the Nucleation of AN Thin Films

direction of B	island density,[a] μm^{-2}	$\Delta(\Delta G^*)$, meV
$B = 0$	0.89	
$B \parallel a_{KAP}$	0.22	9.6 ± 0.3
$B \parallel c_{KAP}$	0.64	2.3 ± 0.4
$B \perp$	0.44	4.9 ± 0.3

[a] The estimates are affected by an error of the order of 5%.

clearly leads to the conclusion that the crystalline islands composing the film possess a strong preferential orientation, which can be estimated as 92% from the ratio between the optical anisotorpy values of the stronger peak; in addition, considering that the maximum absorbance is measured for the light polarized along c_{KAP}, such an axis can be deduced to be aligned to the *b* axis of the AN crystal in the (001) plane, which gives the maximum absorbance.[18] In conclusion, from the optical absorption spectra one can deduce that AN films grown on $(010)_{KAP}$ are crystalline, with $(001)_{AN}$ and $(20\bar{1})_{AN}$ as most probable contact planes. An external magnetic field applied during OMBD does not change the contact plane, whereas, when it is aligned with the c_{KAP}, it makes the AN crystallites align with the $b_{AN} \parallel c_{KAP}$; in all other field configurations the films show a (nearly) random orientation of the crystalline nuclei. Finally, given the same deposition time, in the presence of the magnetic field a lower amount of material gets deposited on the substrate.

A deep study of the same films has been performed by AFM, which gives insights on their morphology and surface structure, providing definitive results and a strong support to the above conclusions. Concerning the morphology, the presence of small crystallites (islands) is a common feature of the AN film growth, where the island density number is observed to display a strong dependence on the direction of the applied magnetic field. Table 1 reports the values of the island density number estimated with AFM averaging over several images. For any direction of the magnetic field the island density number is lower with respect to the case with $B = 0$. Moreover, such a decrease is different for different configurations of the magnetic field, the strongest effect being observed when $B \parallel a_{KAP}$. The number of nuclei observed at the end of the deposition depends on thermodynamical parameters (defining, e.g., the size of the critical nucleus) and on the nucleation kinetics. A variation of the island density number observed in films deposited under the same conditions can be ascribed directly to a variation of the energy barrier for nucleation ΔG^* (neglecting possible variations in the deposition rate at the substrate level (supersaturation) induced by F_B). Because[10] $J = A \exp(-\Delta G^*/k_B T)$, where J is the nucleation rate (number of nuclei formed per unit surface and unit time), A is a kinetic constant, T is the substrate temperature, and k_B is the Boltzmann constant, by assuming a linear dependence of the island density with deposition time, the variation of the island density for films deposited with (n) and without (n_0) magnetic field can be related to the variation of the energy barrier for nucleation $\Delta(\Delta G^*)$:

$$\Delta(\Delta G^*) = k_B T \ln\left(\frac{n_0}{n}\right) \tag{3}$$

The $\Delta(\Delta G^*)$ values calculated from eq 3 are also reported in Table 1. All these values are positive, indicating an increment of the energy barrier due to the presence of a magnetic field, as expected being AN diamagnetic.

To quantitatively determine the effect of the magnetic field in driving the film growth, it is essential to investigate the orientation of the AN crystallites formed on the surface of KAP and to compare the results with those deduced from the optical spectra in Figure 2. Figure 4a reports an AFM image of a polyhedral AN crystallite grown under a magnetic field parallel to c_{KAP}, whereas Figure 4b shows a model of the crystal morphology drawn combining low index faces of the AN crystal structure[16] and the typical shape of bulk AN crystals.[17] The comparison of the model with the crystal shape of the faceted crystallite in Figure 4a shows that the crystallites exhibit the $(001)_{AN}$ face as the contact plane with KAP, in full agreement with the optical spectroscopy data, which suggested this plane as one of the most probable two. Moreover, this crystallite is oriented in such a way that $b_{AN} \parallel c_{KAP}$. To obtain the complete assessment of these results, high resolution AFM measurements were performed probing the top surface of the same crystallite and a typical image is reported in Figure 4c. The image contrast after noise filtering reflects closely the corrugation pertaining to the $(001)_{AN}$ plane. Indeed, the unit cell parameters extracted from the high-resolution images are $a = 8.6 \pm 0.3$ Å and $b = 6.0 \pm 0.3$ Å, in excellent agreement with the a and b parameters of the single-crystal structure of AN.[16]

The same procedure has been employed for the determination of the orientation of the AN islands grown on KAP under different orientations of the magnetic field, to be compared with an optical anisotropy close to that of the single crystal observed in the case of $B \parallel c_{KAP}$ during growth, and with a nearly complete optical isotropy in all other cases. Figure 3 shows some representative images of the films grown for different configurations of the magnetic field. For the present AFM study, several images are collected for each sample and all the observed crystallites considered, so that the results are statistically meaningful. In all cases the contact plane of AN is found to be the $(001)_{AN}$. In the case of $B = 0$ or $B \perp$, crystallites are oriented with equivalent probability either with $b_{AN} \parallel c_{KAP}$, or $b_{AN} \parallel [101]_{KAP}$, or $b_{AN} \parallel [10\bar{1}]_{KAP}$. In the case of $B \parallel c_{KAP}$ all the observed crystallites are oriented with $b_{AN} \parallel c_{KAP}$, whereas in the case of $B \parallel a_{KAP}$ they possess two preferential orientations, with $b_{AN} \parallel [101]_{KAP}$ or $b_{AN} \parallel [10\bar{1}]_{KAP}$. These findings agree well with the above optical results, a strong macroscopic anisotropy being observed only for the samples with strongly oriented crystallites, whereas isotropy arising from the average response of differently oriented crystallites for all other samples.

When substrate and overlayer lattices are highly incommensurate, as in the case of AN/KAP, the contact plane is usually represented by a densely packed, molecularly flat surface. This provides the strongest adhesion of AN on KAP, despite the absence of any epitaxial matching. The (001) plane of AN, which is also a natural cleavage plane of the crystal, is indeed a surface with a very low corrugation, exposing the extremities of the molecules packed in a herringbone motif. The $(001)_{AN}$ plane has always been observed as the contact plane of the crystalline domains, independently of the presence of a magnetic field.

The results discussed above can be fully interpreted by considering the lowering of the energy barrier for nucleation due to the orientation of the crystallites along directions that minimize the energy increment due to the magnetic contribution. Because we do not observe a change of the contact plane when changing the direction of B, we can deduce that a possible decrease of the nucleation energy, reached by orienting the crystals in such a way that the lowest susceptibility is always parallel to B, would result in a too large decrease of the adhesion energy (see eq 2). When the magnetic field is perpendicular to the substrate plane, it forms an angle ζ to the x direction, $90° - \zeta$ to the y direction, and 90° to the z direction (see Figure 1b,c). In this configuration the "effective" magnetic susceptibility of AN induced by the magnetic field can be evaluated by projecting the field along the principal axes of the susceptibility tensor, as sketched in Figure 1c, and then applying eq 1; for this case, it gives $\chi_x \cos^2(\zeta) + \chi_y \sin^2(\zeta) = -9.02 \times 10^{-6}$ for *any* azimuthal orientation of the crystals. As a consequence, the geometry with $B \perp$ affects only the nucleation rate but it does not select a preferential azimuthal orientation of nuclei. When B is applied along the a_{KAP}, the b axis of all AN crystals, parallel to $[10\bar{1}]_{KAP}$ or $[101]_{KAP}$, forms an angle of 34° to the direction of B; then $\theta = 34°$, $\xi = 56°$, and $\phi \approx 10°$ (see Figure 1c) and, following the same arguments as for the previous magnetic field orientation, the effective susceptibility of the crystal gives $\chi_x \sin^2(\phi) + \chi_y \cos^2(\xi) \cos^2(\phi) + \chi_z \cos^2(\theta) = -13.34 \times 10^{-6}$. In this configuration, with respect to the case of $B = 0$ or $B \perp$, crystals with $b \parallel c_{KAP}$ are totally absent. If such crystallites were present, the susceptibility induced by the magnetic field would be $\chi_x \sin^2(\phi) + \chi_y \cos^2(\phi) = -16.19 \times 10^{-6}$ (calculated from $\theta = 90°$, $\xi = 0°$, and $\phi = 26.6°$), which is sufficiently higher than in the previous case to prevent the nucleation of crystals with this orientation. Finally, when B is applied along the c axis of KAP, the b axis of all AN crystals is parallel to B. In this case, the susceptibility is exactly $\chi_z = -9.05 \times 10^{-6}$. Hence, bearing in mind the previous results, this value is much lower and prevents the growth of crystals with any other azimuthal orientation. It must be noted that the

trend of the calculated effective susceptibilities for the three different configurations of the magnetic field reflects that of the nucleation densities reported in Table 1, fully validating our thermodynamical model for nucleation in the presence of a magnetic field.

Conclusions

Evidence of the effect of a static magnetic field on the growth of thin films of AN by OMBD is found, originating from their diamagnetic anisotropy. A strong effect is observed, which combines the influence of the magnetic field with the orienting properties of the KAP substrate, allowing us to obtain an almost completely (more than 90%) oriented film when $B \parallel c_{KAP}$. The results are perfectly consistent in terms of morphology, structure, and optical behavior of the films and can be fully justified starting from the known diamagnetic properties of AN; this suggests the magnetic field as a powerful tool for driving film growth, especially when changing other growth conditions no substantial effects are achieved.

Acknowledgment. The financial support of the National Scientific Program Cofin2002 is kindly acknowledged.

References and Notes

(1) Forrest, S. R. *Chem. Rev.* **1997**, *97*, 1793.
(2) Wakayama, N. I. *Cryst. Growth Des.* **2003**, *3*, 17 and references therein.
(3) Fujiwara, M.; Fukui, M.; Tanimoto, Y. *J. Phys. Chem. B* **1999**, *103*, 2627.
(4) Fujiwara, M.; Chidiwa, T.; Tanimoto, Y. *J. Phys. Chem. B* **2000**, *104*, 8075.
(5) Kawai, T.; Iijima, R.; Yamamoto, Y.; Kimura, T. *J. Phys. Chem. B* **2001**, *105*, 8077.
(6) Yin, D.-C.; Wakayama, N. I.; Wada, H.; Huang, W.-D. *J. Phys. Chem. B* **2003**, *107*, 14140.
(7) (a) Mori, T.; Mori, K.; Mizutani, T. *Thin Solid Films* **1999**, *338*, 300. (b) *Thin Solid Films* **2000**, *366*, 279. (c) *Thin Solid Films* **2001**, *393*, 143.
(8) Ji, Z. G.; Wong, K. W.; Tse, P. K.; Kwork, R. W. M.; Lau, W. M. *Thin Solid Films* **2002**, *402*, 79.
(9) Morrish, A. H. *The Physical Principles of Magnetism*; IEEE Press: New York, 2001.
(10) Mutaftschiev, B. *The Atomistic Nature of Crystal Growth*; Springer Series in Materials Science: Berlin, 2001.
(11) Sigma Aldrich.
(12) Tubino, R.; Borghesi, A.; Dalla Bella, L.; Destri, S.; Porzio, W.; Sassella, A. *Opt. Mater.* **1998**, *9*, 437.
(13) Eremina, T. A.; Furmanova, N. G.; Lakakhova, L. F.; Okhrimenko, T. M.; Kuznetsov, V. A. *Crystallogr. Rep.* **1993**, *38*, 554.
(14) Campione, M.; Cartotti, M.; Pinotti, E.; Sassella, A.; Borghesi, A. *J. Vac. Sci. Technol. A* **2004**, *22*, 482.
(15) Landolt-Börnstein, New Series II/16, p 403.
(16) Brock, C. P.; Dunitz, J. D. *Acta Crystallogr.* **1990**, *B46*, 795.
(17) Groth, P. *Chemische Kristallographie*; Wilhelm Engelmann: Leipzig, 1906−1919; Vols. 1−5.
(18) Clark, L. B.; Philpott, M. R. *J. Chem. Phys.* **1970**, *53*, 3790.